Security
of Infocommunication Systems
and Internet of Things

2024 Vol 2, No 2

https://doi.org/10.31861/sisiot2024.2.02008

Received 08 December 2024; revised 19 December 2024; accepted 23 December 2024; published 30 December 2024

# Development of *n-TiN/p-CdTe/n-CdTe* Phototransistors for Use in a Networked Digital Light Sensor

**Ivan Orletsky[1], Mariia Ilashchuk[1], Sergiy Nichy[1,*] and Bohdan Nichy[2]**

[1]Department of Electronics and Power Engineering, Yuriy Fedkovych Chernivtsi National University, Chernivtsi, Ukraine
[2]Department of Radio Engineering and Information Security, Yuriy Fedkovych Chernivtsi National University, Chernivtsi, Ukraine

*Corresponding author (E-mail: s.nichyi@chnu.edu.ua)

**ABSTRACT** In this work, the mode of production by reactive magnetron sputtering of *n-TiN/p-CdTe/n-CdTe* heterostructures, which have the properties of a phototransistor with an unconnected (floating) base, is investigated. It is shown that in the structure of n-*TiN/p-CdTe/n-CdTe* at reverse voltage at the collector junction of *p-CdTe/n-CdTe* under conditions of irradiation close to AM1 from the side of the *n-TiN* emitter, the phenomenon of amplification of the collector photocurrent by the direct current of the directly switched on is observed of the *n-TiN/p-CdTe* heterojunction. A forward voltage is applied to the *n-TiN/p-CdTe* heterojunction due to the positive charge of the *p-CdTe* base during illumination. Photoelectric phenomena during illumination of the *n-TiN/p-CdTe/n-CdTe* heterostructure were analyzed. The purpose of this work is to evaluate the practical use of the newly created *n-TiN/p-CdTe/n-CdTe* heterostructure in the phototransistor mode of operation to create an illumination sensor with a digital interface for use in network control and management systems. The possibility of using the manufactured transistor as a digital illuminance sensor for large values of light flux is substantiated. The phototransistor was used as the primary converter for the microcontroller, which includes a functional block of the operational amplifier. The phototransistor and the operational amplifier together implement the photocurrent-voltage converter system. This solution allows you to use the internal operational amplifier of microcontrollers with a unipolar power supply. The linearization of the transfer characteristics of the phototransistor allows you to use microcontrollers with low computing power. It was established that the transfer characteristics are closer to linear ones with an increase in the voltage between the collector and the emitter of the phototransistor. The sensor device using the developed transistor was assembled on a PIC16F1713 series microcontroller, which contains an operational amplifier that allows the implementation of a universal synchronous-asynchronous receiver/transmitter digital interface for transmitting the measured light flux data. Implementing a wireless light sensor on the GB2530 module, which is based on the system on a chip CC2530 allows you to get a mobile device. Data exchange on the airwaves takes place in accordance with the IEEE 802.15.4 standard.

**KEYWORDS** phototransistor, heterostructure, microcontroller, illuminance.

## I. INTRODUCTION

Modern photo devices based on semiconductor structures make it possible to use the energy of natural light in various aspects. The creation of new semiconductor photo devices is aimed at increasing their sensitivity, reducing production costs. This work presents the possibilities of applied use of the created heterojunctions on promising *n-TiN/p-CdTe/n-CdTe* structures. Having the properties of a phototransistor, this structure can be used as a light sensor on the basis of which it is possible to create devices used in solar energy, environmental control of greenhouses, office, hospital premises, etc. The purpose of this work is to assess the practical use of the newly created heterostructure *n-TiN/p-CdTe/n-CdTe* in the phototransistor mode of operation to create an illumination sensor with a digital interface.

Thin films of titanium nitride (*TiN*) have physical properties that contribute to wide application in the creation of electronic devices. They are used in photovoltaic devices as an electrode material for dye solar cells [1], in ultra-thin organic photoconverters [2], as selective contacts of organic-inorganic hybrid solar cells [3], in plasmonic silicon solar cells [4]. A wide band gap $E_g \approx 3.4$ eV and a low electrical resistivity $\rho \approx 0.4\ \Omega\cdot$cm [5,6] make it possible to manufacture photosensitive *TiN/p-CdTe* heterojunctions [7], in which the low-resistance front layer of *TiN* provides a high degree of penetration of light quanta to absorbing layer. The high electrical conductivity of *TiN* films contributes to the efficient removal of charge carriers into the external electric circuit. A wide range of values of the energy parameter work function 3.5 – 4.4 eV [8-11] of *TiN* films obtained under different conditions is used in semiconductor structures to create ohmic contacts to *n-CdS* [8], *n-Si* [12] and gate electrodes of *MOS* structures based on silicon [13].

In addition to ohmic contacts with semiconductors, *TiN* thin films are capable of forming heterojunctions with diode properties. This is manifested when they are applied to semiconductor materials *Ge* and *Si*, and to crystals of compounds $Hg_3In_2Te_6$ [14] and *InSe* [15]. When using substrates with hole-type electrical conductivity, the energy parameters and electrical properties of anisotype heterojunctions *TiN/Ge*, *TiN/p-Si*, *TiN/p-*$Hg_3In_2Te_6$, *TiN/p-InSe* agree satisfactorily with models that use constants at the heterojunction low (~ 3.69 – 3.75 eV) electron affinity values for films. When applying these models for isotypic heterojunctions, for example *TiN/n-Si*, discrepancies with experimental data arise. Based on the heterocontact model with unchanged energy parameters *TiN/n-Si* should be ohmic with the formation of an electron-enriched region in *n-Si*. Experimental data indicate non-ohmic characteristics of the *TiN/n-Si* heterojunction. A similar situation occurs when analyzing heterocontacts *TiN/n-CdTe*. In this work, the results of the study of electrical properties are analyzed and the practical use of the newly created heterostructure is evaluated *n-TiN/p-CdTe/n-CdTe* in the phototransistor mode of operation to create an illumination sensor with a digital interface.

## II. PRODUCTION TECHNOLOGY AND PROPERTIES OF STRUCTURES *n-TiN/p-CdTe/n-CdTe*

For the manufacture of *n-TiN/p-CdTe/n-CdTe* structures, substrates of *n*-type cadmium telluride crystals of electrical conductivity were used. At a temperature of 295 K, they had a resistivity $\rho \approx 1$ Ohm·cm and a concentration of charge carriers $n = 1.5 \cdot 10^{16}$ cm$^{-3}$. The location of the Fermi level in the band gap of cadmium telluride $E_C - E_F = 0.1$ eV.

Thin films of *TiN* were deposited by reactive magnetron sputtering at a constant voltage of a titanium target in a mixture of nitrogen and argon gases on a freshly chipped substrate of crystalline cadmium telluride measuring 5mm×5mm×0.3mm using a universal vacuum unit Leybold - Heraeus L 560. Short-term etching of the surface with argon ions was used to clean the target and substrates. With this mode of deposition, the *TiN* film possessed *n*-type electrical conductivity, the specific electrical conductivity at $T = 295$ K was $\sigma = 0.17\ \Omega^{-1} \cdot$cm$^{-1}$, the electron concentration $n = 1.7 \cdot 10^{19}$cm$^{-3}$. Before the *TiN* film deposition process, the *n-CdTe* substrates were heated to a temperature of ~ 570 K. Such a temperature effect, due to the high volatility of cadmium, leads to the formation of cadmium vacancies in the near-surface region of the substrates, which contribute to the formation of holes. There is a re-compensation of the conductivity type with the formation of a *p-CdTe* layer in the *n-CdTe* substrate from the *TiN* film growth side.

Contacts to the *TiN* thin film were made by thermal sputtering of indium at a substrate temperature of 423 K. For cadmium telluride substrates, ohmic contacts were made by indium fusion at a temperature of about 180ºC to form a heavily doped *n-CdTe* layer. To construct the energy diagram of the *n-TiN/p-CdTe/n-CdTe* structure, data on the height of the eigenretic barriers at the contacts of *p-CdTe/n-CdTe* and *n-TiN/p-CdTe* were used, which were obtained from the experimental data of the study of voltaic faradic characteristics. For homotransition *p-CdTe/n-CdTe*, which is formed in the *n-CdTe* substrate $q\varphi_{k2} = 1.07$ eV. For heterojunction *n-TiN/p-CdTe* $q\varphi_{k1} = 1.1$ eV. The electron concentration in the *n-CdTe* substrate is $n = 1.5 \cdot 10^{16}$ cm$^{-3}$. To determine the depth of the Fermi level in *n-CdTe* $\delta_2 = 0.1$ eV, the relation for non-degenerate semiconductors was used:

$$E_C - E_F = \delta = kT \cdot ln\left(2 \cdot \left(\frac{2\pi m_n kT}{h^2}\right)^{3/2} \cdot \frac{1}{n}\right), \quad (1)$$

where $m_n$ is the effective mass for electrons in *CdTe* ($m_n = 0.096 \cdot m_0$), $E_F$ is the energy for the Fermi level of the band gap. Eg. (2) can be used in the following form:

$$E_C - E_F = \delta = kT \cdot ln\left(\frac{N_C}{n}\right), \quad (2)$$

where $N_C = 7.41 \cdot 10^{17}$ cm$^{-3}$ is the effective value of the density of states in the conduction band of *n-CdTe*.

The concentration of holes in *p-CdTe* is from $p = 1.71 \cdot 10^{15}$ cm$^{-3}$ near the contact *n-TiN/p-CdTe* up to $p = 9.12 \cdot 10^{14}$ cm$^{-3}$ near the *p-CdTe/n-CdTe* contact. That is, there is a concentration gradient of acceptors in the base region. To determine the depth of the Fermi level in *p-CdTe* $\delta_1 = 0.23 - 0.33$ eV used an expression for non-degenerate semiconductors in the form:

$$E_F - E_V = \delta = kT \cdot ln\left(2 \cdot \left(\frac{2\pi m_p kT}{h^2}\right)^{3/2} \cdot \frac{1}{p}\right), \quad (3)$$

or in the form of:

$$E_F - E_V = \delta = kT \cdot ln\left(\frac{N_V}{p}\right), \quad (4)$$

where $N_V = 5.16 \cdot 10^{18}$ cm$^{-3}$, $m_p = 0.35 \cdot m_0$.

The output functions for electrons $A_n$ or $A_p$ for semiconductors *n-CdTe* and *p-CdTe* were calculated according to the ratios:

$$A_n = \chi_1 + \delta_n; \quad A_n = \chi_2 + (E_{g2} - \delta_p). \quad (5)$$

Thicknesses of hole-depleted regions of the base region $d_1$ and $d_2$ were calculated by the expression:

$$d_{1,2} = \sqrt{\frac{2\varepsilon_0 \varepsilon_S \phi_{k1,k2}}{qN_a}}. \quad (6)$$

The energy diagram of the *n-TiN/p-CdTe/n-CdTe* structure is shown in Fig. 1.

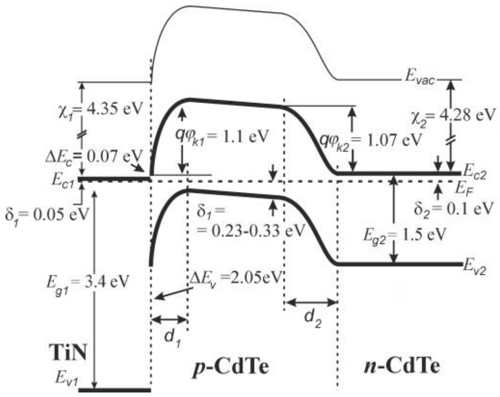


**FIG. 1.** Energy diagram of the *n-TiN/p-CdTe/n-CdTe* structure.

According to experimental data, the affinity of *TiN* is 4.35 eV. Thickness $d_1 = 0.83$ µm, $d_2 = 1.13$ µm. Actually received $\delta_1 = 0.223$ eV (at $p = 1.71 \cdot 10^{15}$ cm$^{-3}$, $N_V = 5.16 \cdot 10^{18}$ cm$^{-3}$, $m_p = 0.35 \cdot m_0$). Used in the construction of $\delta_1 = 0.33$ eV (corresponds to $p = 1.5 \cdot 10^{13}$ cm$^{-3}$) agrees well with the parameters of the diagram.

The obtained value of electron affinity correlates well with works: according to *TiN/Ge* 4.3 eV [14], MDP structures *TiN/SiO$_2$/Si/Al* 4.2 – 4.5 eV [13], *TiN/CdS* 3.5 – 4.4 eV [8]. Work was determined on the TIR structures of *TiN/SiO$_2$/Si/Al* function 4.2 – 4.5 eV based on the volt-farad characteristics similarly [15] (on the voltage of flat zones).

## III. PHOTOTRANSISTOR PROPERTIES OF THE STRUCTURE *n-TiN/p-CdTe/n-CdTe*

Fig. 2 shows the polarity of switching on the *n- TiN/p-CdTe/n-CdTe* structure for observing phototransistor properties. The *n-TiN* film is the emitter region of the phototransistor. The base region is *p-CdTe*. An external contact is not connected to it. That is, the *n-TiN/p-CdTe/n-CdTe* photo transistor has a floating base region. The *n-CdTe* crystal plays the role of a collector.

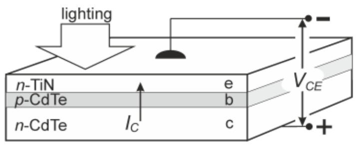


**FIG. 2.** Polarity of switching on the *n-TiN/p-CdTe/n-CdTe* structure to observe phototransistor properties.

Fig. 3 shows the energy diagram of photocurrent amplification in the *n-TiN/p-CdTe/n-CdTe* structure due to the injection of electrons from the emitter region. When illuminated, electron-hole pairs are generated in the *p-CdTe* base and the *p-CdTe/n-CdTe* transition. The generated electrons go to *n-CdTe*, and the generated holes collect in the *p-CdTe* base. The process is analogous to applying a positive potential to the base. The barrier height for *n-TiN* conduction band electrons decreases and they flow through the *p-CdTe* base into the *n-CdTe* collector region.

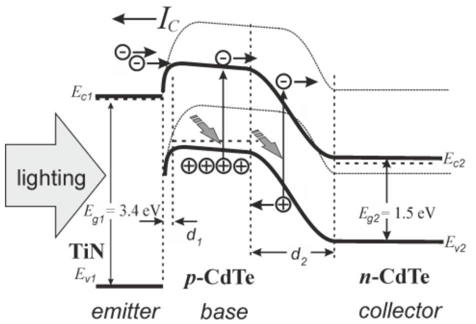


**FIG. 3.** Amplification of the photocurrent in the *n-TiN/p-CdTe/n-CdTe* structure due to the injection of electrons from the emitter region.

*I-V* characteristics phototransistor heterostructures *n-TiN/p-CdTe/n-CdTe* with integral irradiation close to the conditions of AM1.5 100 mW/cm$^2$ (corresponds to 85,000 lx and less to 20,000 lx from the side of the *n-TiN* film reveal the internal amplification of the photocurrent $I_C$ up to 0.5 mA at displacements between the collector and the emitter of ~ 5 V (Fig. 4). The study of the *I-V* characteristics of the *TiN/p-CdTe/n-CdTe* heterostructures was carried out using a semiconductor device parameter meter L2-56. A halogen lamp with a light flux concentrator was used as a light source. Yu116 luxmeter was used to measure the illumination. During the study of the *I-V* characteristics, the temperature of the heterostructure was constantly monitored, which was at 20 °C.

Based on the developed and obtained phototransistor *n-TiN/p-CdTe/n-CdTe* has implemented an illumination sensor with digital transmission of illumination value data. It is also promising to implement both wired and wireless lighting sensors for use in the corresponding sensor networks and Internet of Things.

## IV. PHOTOTRANSISTOR SENSOR

The scheme of the primary converter for determining the level of illumination is based on the electro-optical properties of the phototransistor of the *n-TiN/p-CdTe/n-CdTe* structure. To convert the amount of illumination into an electrical signal (voltage or current) with the help of a phototransistor, phototransistor circuits with a common emitter or a common collector are used. The same photophysical processes of converting photon energy into an electrical value occur in these phototransistor switching schemes. In addition, the requirement for the process of illumination from the emitter region and the design of the transistor indicate the optimality of using a circuit with a common emitter.

To implement a sensor with a digital interface, it is necessary to process the signal from the phototransistor with a microcontroller. If the formula $V = f(E)$ (Fig. 4) is used to determine the illumination (where *I*, *V*, *E* are the current, voltage, and illumination values, respectively), then significant computing power must be used due to the nonlinearity of the phototransistor *I-V* characteristic. If the dependence $I = f(E)$ (Fig. 5) is used, then due to the almost linear dependence of the photocurrent on the illumination, the computing power will be much lower.

Analog-to-digital converters (ADC) implemented in microcontrollers convert analog voltage into digital code, so it is necessary to convert the functional dependence $I=f(E)$ into a linear dependence $V=f(E)$ using a current-voltage converter. In general, the process of converting the analog value of illumination into a numerical code at the digital output of the sensor will correspond to the block diagram in Fig. 6.

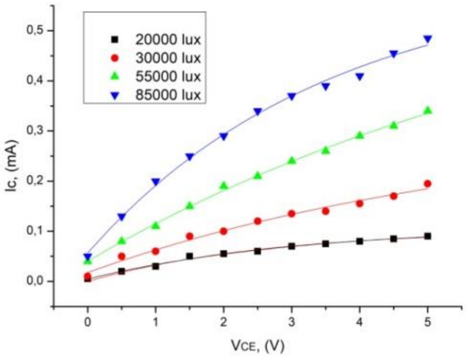


**FIG. 4.** Typical dependences of the collector current $I_C$ on the collector-emitter voltage $V_{CE}$ and different illumination levels *E* (halogen lamp) for the *n-TiN/p-CdTe/n-CdTe* structure.

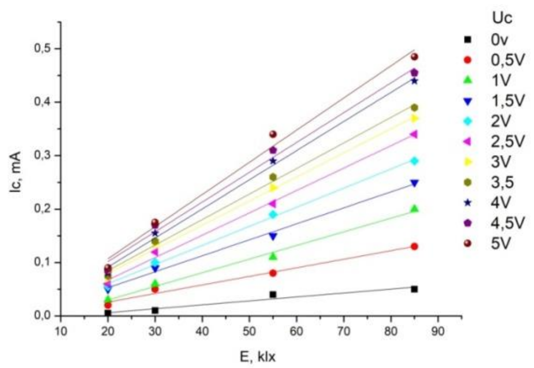


**FIG. 5.** Typical dependences of the collector current $I_C$ on the level of illumination *E* (halogen lamp) and voltages $V_{CE}$ for the *n-TiN/p-CdTe/n-CdTe* structure.

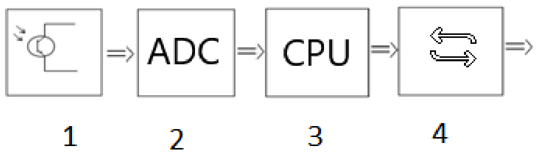


**FIG. 6.** Block diagram of the process of obtaining a digital code of the illumination level: 1 – current-voltage converter, 2 – ADC, 3 – computing unit (microprocessor), 4 – digital interface (wired/wireless).

According to the proposed concept of creating a digital light sensor on phototransistors of the *n-TiN/p-CdTe/n-CdTe* structure it is necessary to use microcontrollers that contain an operational amplifier block, for example, the PIC16F1713 series [16]. It is also possible to create wireless sensor lights on the system on a chip (SoC) module GB2530 [17, 18]. The current-voltage converter [19] block on the microcontroller operational amplifier is implemented according to the diagram in Fig. 7.

The voltage on the collector of phototransistor VT1 is set by resistors R1 and R2, which are connected to the non-inverting input *OPAin+* of the operational amplifier block of the microcontroller. Phototransistor VT1 and resistors R3 and R4 in the circuit of the inverting input *OPAin-* operational amplifier OPA converts the photocurrent into a directly proportional value of the voltage that is fed from the output *OPAout* to the input output of the analog-to-digital converter block *ADCin* microcontroller.

In this case, the general form of the functional transformation for obtaining the numerical value of illumination into a digital code will be described by the following mathematical formulas:

$$E = kI = k\frac{U_{OPA}}{R3+R4} = k\frac{U_{ADC}}{R3+R4} = \frac{k}{R3+R4}\cdot\frac{U_{REF}}{2^n-1}\cdot N, \quad (7)$$

where, $V_{REF}$ is the value of the reference voltage, $n$ is the *ADC* bit rate, $N$ is the numerical value of the illumination in the binary numbering system, $V_{OPA}$ is the voltage from the output of the operational amplifier, $V_{ADC}$ is the voltage at the ADC input. As shown by the formula and graphs in Fig. 4, the proportionality coefficient $k = E/I$ can introduce the largest errors during the conversion of values. Table 1 shows the calculated values of the coefficient $k$ at the largest deviations of the photocurrent from the illumination according to Fig. 4.

Deviation by more than 20% of the coefficient $k$ at values of $V_C \leq 1$ V and $E = 20000$ lx due to the significant non-linearity of the volt-ampere characteristics of the *p-n* junctions of the transistor at low collector-emitter voltages. At the values of $V_C \geq 1.5$ V and $E > 20000$ lx deviation of the proportionality factor $k$ is within ±10% and is quite acceptable for use as a light sensor for large light levels. If you plot the graphs with dependencies $E = f(I)$ (Fig. 8), then to make a linear relationship with the help of a polynomial of the form $Y = A + BX$, you can get the necessary values of $A$ and $B$ to calculate the value of illumination $E$ at the measured currents $I$, for example, using software package ORIGIN. If you define $q$ as a coefficient that determines the voltage value on the collector $V_C = q\cdot V_{DD} = q\cdot V_{REF} = V_{OPAin+}$ $(q < 1)$, then the price of a unit of the numerical value of illumination at the output of the ADC is determined by the formula

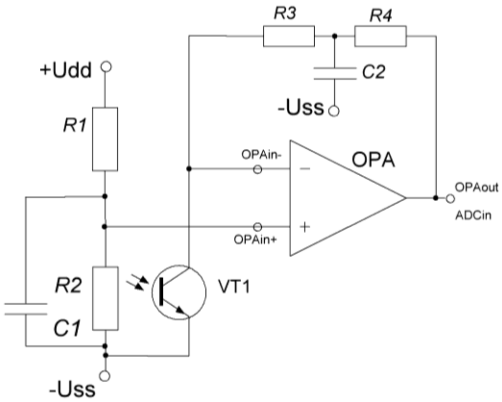


**FIG. 7.** Scheme of implementation of the current-voltage converter of the illumination sensor using the operational amplifier unit of microcontrollers: OPAin- (7pin PIC16F1713, 12 pin GB2530), OPAin+ (6pin PIC16F1713, 13 pin GB2530), OPAout (3pin PIC16F1713, 11 pin GB2530), ADCin (2pin PIC16F1713, 10 pin GB2530).

$$\frac{\Delta E}{(2^n-1)-q(2^n-1)} = \frac{\Delta E}{(2^n-1)(1-q)}. \quad (8)$$

It follows from this formula that q should go to zero, but as can be seen from Fig. 4 and Table 1 at small $V_C$ values the transistor is characterized by a significant nonlinear dependence of the photocurrent on illumination.

Then, in this case, the general form of the functional transformation for obtaining the numerical value of illumination into a digital code will be described by the following mathematical formulas:

$$E = A + BI = A + B\frac{V_{OPA} - V_{OPAin+}}{R3 + R4} =$$

$$= A + B\frac{V_{ADC} - V_{OPAin+}}{R3 + R4} =$$

$$= A + \frac{B}{R3+R4}\cdot\frac{V_{REF}}{2^n-1}(N - q(2^n - 1)), \quad (9)$$

where, $V_{REF}$ $(V_{REF}=V_{DD})$ is the value of the reference voltage, $n$ is the ADC bit rate, $N$ is the numerical value of the illumination in the binary numbering system, $V_{OPA}$ is the voltage from the output of the operational amplifier, $V_{ADC}$ is the voltage at the ADC input.

**TABLE 1.** The value of the proportionality coefficient *k*.

| *E* | *Vc*=0 V | *Vc*=0.5V | *Vc*=1V | *Vc*=1.5V | *Vc*=2V | *Vc*=2.5V | *Vc*=3V | *Vc*=3.5V | *Vc*=4V | *Vc*=4.5V | *Vc*=5V |
|---|---|---|---|---|---|---|---|---|---|---|---|
| 20000 | 4000.0 | 1000.0 | 666.7 | 400.0 | 363.6 | 333.3 | 285.7 | 266.7 | 250.0 | 235.3 | 222.2 |
| 30000 | 3000.0 | 600.0 | 500.0 | 333.3 | 300.0 | 250.0 | 222.2 | 214.3 | 193.5 | 176.5 | 171.4 |
| 55000 | 1375.0 | 687.5 | 500.0 | 366.7 | 289.5 | 261.9 | 229.2 | 211.5 | 189.7 | 177.4 | 161.8 |
| 85000 | 1700.0 | 653.8 | 425.0 | 340.0 | 293.1 | 250.0 | 229.7 | 217.9 | 193.2 | 186.8 | 175.3 |

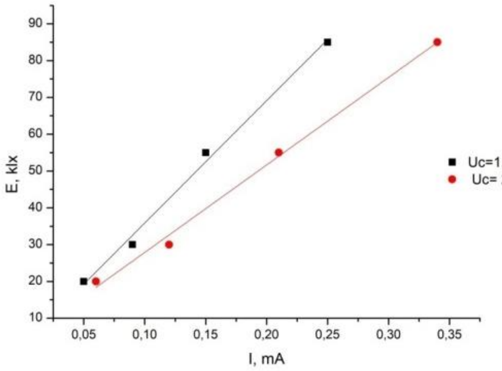


FIG. 8. Reconstructed dependences of the illumination level $E$ on the collector current $I_C$ of the transistor at voltage values $V_{CE}$.

Linearization is carried out in Fig. 8 for two $Vc$ voltage values of 1.5 V and 2.5 V, because the light sensor was investigated at supply voltages of 3 V (CC2530) and 5 V (PIC16F1713/6). Therefore, we chose $q = 0.5$. Linearization coefficients $A = 2.599 \cdot 10^3$ and $B = 332.599 \cdot 10^3$ for $V_C = 1.5$ V, and $A = 4.1 \cdot 10^3$ and $B = 237.774 \cdot 10^3$ for $V_C = 2.5$V. In both cases, the maximum deviation of the measured $E$ values from the calculated values did not exceed ±11%. The values of the components are as follows R1 = R2, $q$ = 0,5.

When using PIC16F1713, the calculated sum of R3+R4 was equal to 7.35 kΩ, so R3 = R4 = 3.6 kΩ. Therefore, the calculation formula for calculating the illumination by the microcontroller processor core was as follows:

$$E = (4{,}1 + \frac{237{,}7}{7{,}2} \cdot \frac{5}{2^{10}-1}(N - 0{,}5(2^{10} - 1)) \cdot 10^3. \quad (10)$$

When using GB2530, the calculated sum of R3+R4 was equal to 6 kΩ, so R3 = R4 = 3 kΩ. Therefore, the calculation formula for calculating the illumination by the microcontroller processor core was as follows:

$$E = (2{,}599 + \frac{332{,}6}{6} \cdot \frac{3}{2^{12}-1}(N - 0{,}5(2^{12} - 1)) \cdot 10^3. \quad (11)$$

The sensor device using the developed transistor assembled according to the diagram in Fig. 7 was assembled on a microcontroller series PIC16F1713/6, which contains an operational amplifier. Algorithm of operation of the microcontroller involves data exchange via the USART digital interface, data exchange in the format shown in Fig. 9.

a)

| Start byte | Command byte | Stop byte |
|---|---|---|

b)

| Start byte | Data field | Stop byte |
|---|---|---|

FIG. 9. Digital interface field formats: (a) format of sensor request commands, (b) format of output data from the sensor.

Command and data fields are transmitted in ASCII format, without a checksum:

- Start byte of command 01h;
- Start data byte 02h;
- Stop byte of command and data FFh;
- Command byte:
  - 11h – start measurements;
  - 12h – transfer the last measured data;
  - 13h – start 10-fold measurements;
  - 14h– transfer the averaged data.
- Format data field
  - 1 byte - tens of thousands.
  - 2 byte - thousands.
  - 3 byte - hundreds.
  - 4 byte - tens.
  - 5 byte - units.

Implementing a wireless light sensor on the GB2530 module, the basis of which is the SoC CC2530 allows you to get a mobile device. This solution allows you to use the internal operational amplifier of the CC2530 with unipolar power supply. Data exchange on the airwaves takes place in accordance with the IEEE802.15.4 standard. One of the conditions for safe data storage in IEEE802.15.4 networks is the stability of packet transmission in accordance with the format shown in Fig. 9. Research was conducted to find the greatest distance at which our packets are not lost. According to the characteristics of the CC2530, the sensitivity of the receiver in it is at the level of -97 dBm [17]. The power of the transmitter is set by software. The maximum value that can be set is 4.5 dBm. To determine the maximum range of reliable reception, we used a network traffic analyzer and the program "SmartRF Packet Sniffer". Using the field indicators of the level of the input signal determined with the help of the analyzer, we built a graph (Fig. 10) of the dependence of the level of the received signal on the distance between the transmitter (developed device) and the receiver (network analyzer) at the level of direct visibility at a height of 1.2 m.

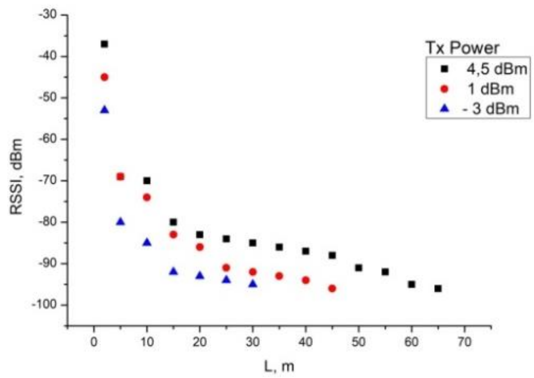


FIG. 10. Graph of the dependence of the signal level at the receiver input on the distance to the transmitter.

The analysis of the measurement results shows that the range of stable reception is 65 m in line of sight. At the studied levels of the specified output power of the CC2530 signal (4.5 dBm, 1 dBm and -3 dBm), packet losses began to be observed at a distance of 70 m, 50 m and 35 m, respectively.

## V. CONCLUSION

The proposed technology for obtaining a photosensitive transistor structure has prospects for further improvement. Calculations and the experimental part of the work indicate the possibility of using the *n-TiN/p-CdTe/n-CdTe* structure to build a digital light sensor based on single-crystal processor systems. Linearization of the transfer characteristics of the phototransistor allows the use of microcontrollers with low computing power. It was established that the transfer characteristics are closer to linear ones with an increase in the voltage between the collector and the emitter of the phototransistor. The sensor device using the developed transistor and PIC16F171 series microcontroller, which contains an operational amplifier, allows to implement a USART digital interface for transmitting the measured light flux data. Implementing a wireless light sensor on the GB2530 module, which is based on the SoC CC2530 allows you to get a mobile device in which data exchange over the air takes place in accordance with the IEEE 802.15.4 standard.

## AUTHOR CONTRIBUTIONS

I.O. – writing (original draft preparation), conceptualization, methodology; M.I. – investigation, resources; S.N. – methodology, investigation, writing (review and editing) B.N. – software, investigation, resources, writing-original draft preparation.

## COMPETING INTERESTS

The authors declare no competing interests.

## REFERENCES


[1] T. Mohan, K.G. Baiju, B. Murali, and D. Kumaresan, "Titanium Nitride Blended Graphene Nanoplatelets as Low-cost and Efficient Composite Counter Electrode for Dye-sensitized Solar Cells," in *2018 IEEE International Conf. on System, Computation, Automation and Networking (ICSCA)*, IEEE, Pondicherry, India, 2018, pp. 1-5.

[2] Z. Khezripour, F.F. Mahani, and A. Mokhtari, "Performance improvement of ultrathin organic solar cells utilizing light-trapping aluminum-titanium nitride nanosquare arrays," *Optical Materials*, vol. 84, pp. 651-657, 2018.

[3] Z. Lu, X. Liu, G. Hou, J. Chen, T. Zhu, J. Xu, and K. Chen, "Doping-Free Titanium Nitride Carrier Selective Contacts for Efficient Organic–Inorganic Hybrid Solar Cells," *ACS Appl. Energy Mater.*, vol. 3, pp. 9208-9215, 2020.

[4] A.E. Khalifa and M.A. Swillam, "Plasmonic silicon solar cells using titanium nitride: a comparative study," *J. Nanophoton.*, vol. 8, pp. 84-98, 2014.

[5] M.M. Solovan, V.V. Brus, E.V. Maistruk, and P.D. Maryanchuk, "Electrical and Optical Properties of TiN Thin Films," *Inorg. Mater.*, vol. 50, no. 1, pp. 46-51, 2014.

[6] H. Jeon, J.-W. Lee, Y.-D. Kim, D.-S. Kim, and K.-S. Yi, "Study on the characteristics of TiN thin film deposited by the atomic layer chemical vapor deposition method," *J. Vac. Sci. Technol. A: Vac. Surf. Films*, vol. 18, pp. 1595-1598, 2000.

[7] M.M. Solovan, V.V. Brus, P.D. Maryanchuk, M.I. Ilashchuk, J. Rappich, N. Nickel, and S.L. Abashin, "Fabrication and characterization of anisotype heterojunctions n-TiN/p-CdTe," *Semicond. Sci. Technol.*, vol. 29, p. 015007, 2014.

[8] A. Didden, H. Battjes, R. Machunze, B. Dam, and R. van de Krol, "Titanium nitride: A new Ohmic contact material for n-type CdS," *J. Appl. Phys.*, vol. 110, p. 033717, 2011.

[9] G.M. Matenoglou, L.E. Koutsokeras, and P. Patsalas, "Plasma energy and work function of conducting transition metal nitrides for electronic applications," *Appl. Phys. Lett.*, vol. 94, p. 152108, 2009.

[10] S. Ishii, S.L. Shinde, W. Jevasuwan, N. Fukata, and T. Nagao, "Hot Electron Excitation from Titanium Nitride Using Visible Light," *ACS Photonics*, vol. 3, pp. 1552-1557, 2016.

[11] A. Naldoni, U. Guler, Z. Wang, M. Marelli, F. Malara, X. Meng, L.V. Besteiro, A.O. Govorov, A.V. Kildishev, A. Boltasseva, V.M. Shalaev, "Broadband Hot-Electron Collection for Solar Water Splitting with Plasmonic Titanium Nitride," *Adv. Opt. Mater.*, vol. 5, p. 1601031, 2017.

[12] X. Yang, W. Liu, M. De Bastiani, T. Allen, J. Kang, H. Xu, E. Aydin, L. Xu, Q. Bi, H. Dang, E. AlHabshi, K. Kotsovos, A. AlSaggaf, I. Gereige, Y. Wan, J. Peng, C. Samundsett, A. Cuevas, and S. De Wolf, "Dual-Function Electron-Conductive, Hole-Blocking Titanium Nitride Contacts for Efficient Silicon Solar Cells," *Joule*, vol. 3, pp. 1314-1327, 2019.

[13] L.P.B. Lima, J.A. Diniz, I. Doi, and J. Godoy Fo, "Titanium nitride as electrode for MOS technology and Schottky diode: Alternative extraction method of titanium nitride work function," *Microelectron. Eng.*, vol. 92, pp. 86-90, 2012.

[14] M.N. Solovan, A.I. Mostovyi, V.V. Brus, E.V. Maistruk, P.D. Maryanchuk, "Electrical and photoelectric properties of n-TiN/p-Hg3In2Te6 heterostructures," *Semiconductors*, vol. 50, pp. 1020-1024, 2016.

[15] I.G. Orletsky, M. Ilashchuk, V.V. Brus, P.D. Marianchuk, M.M. Solovan, and Z.D. Kovalyuk, "Electrical and Photoelectric Properties of the TiN/p-InSe Heterojunction," *Semiconductors*, vol. 50, pp. 334-338, 2016.

[16] Microchip, "PIC16(L)F1713/6. Cost Effective 8-Bit Intelligent Analog Flash Microcontrollers," DS40001726C datasheet, 2013-2018.

[17] Texas Instruments, "CC2530F32, CC2530F64, CC2530F128, CC2530F256. A True System-on-Chip Solution for 2.4-GHz IEEE 802.15.4 and ZigBee Applications," SWRS081B datasheet, Apr. 2009 [Revised Feb. 2011].

[18] Gban Electronsc Technology, "Use CC2530 or CC2531 Chipset ZigBee Module," GB23x-M datasheet, V1.0, 10 Aug. 2013.

[19] Texas Instruments, "An-20 Applications Guide for Op Amps," SNOA621C datasheet, Feb. 1969 [Revised May 2013].


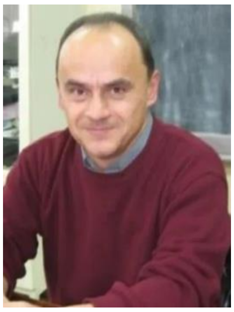


### Ivan Orletsky

In 1990, he graduated from Yuriy Fedkovych Chernivtsi State University (specialty "Semiconductors and Dielectrics"). From 1993 to 1996, he studied at the postgraduate course (specialty – 01.04.10 – "Physics of Semiconductors and Dielectrics"). In 1996, he defended his PhD thesis for the degree of Candidate of Physical and Mathematical Sciences. The subject of his scientific interests includes obtaining and studying the photoproperties of semiconductor materials and devices.

**ORCID ID:** 0000-0001-5202-8353



### Mariia Ilashchuk

In 1971, she graduated from Chernivtsi State University (Department of Semiconductor Materials). Major in Physics.The candidate's thesis was defended in 1984. In 1991, she received the academic title of Senior Research Fellow.She has published over 160 scientific and educational works (including 2 patents, 1 textbook).

**ORCID ID:** 0000-0002-7618-0437

**Sergiy Nichy**

In 1990 he graduated from Chernivtsi State University with a degree in Semiconductors and Dielectrics. Since 1990 he has been a research associate and associate professor at the Department of Semiconductor Microelectronics of Chernivtsi State University. In 1997 he defended his PhD thesis. His research interests include research in the field of primary converters for wireless sensor networks and automation systems.

**ORCID ID:** 0000-0003-2662-9694

**Bohdan Nichy**

In 2020, he graduated from Chernivtsi National University with a master's degree in "Electronic Communications and Radio Engineering". Currently a postgraduate student of the Department of Radio Engineering and Information Security. His scientific interests and research interests include the security of telecommunication networks and systems.

**ORCID ID:** 0009-0001-4855-2053

# Розробка фототранзисторів *n-TiN/p-CdTe/n-CdTe* для використання в мережевому цифровому світловому датчику

**Іван Орлецький[1], Марія Ілащук[1], Сергій Нічий[1,*], Богдан Нічий[2]**

[1]Кафедра електроніки і енергетики, Чернівецький національний університет імені Юрія Федьковича, Україна
[2]Кафедра радіотехніки та інформаційної безпеки, Чернівецький національний університет імені Юрія Федьковича, Україна

*Автор-кореспондент (Електронна адреса: s.nichyi@chnu.edu.ua)

**АНОТАЦІЯ** В даній роботі досліджено режим виготовлення методом реактивного магнетронного напилення гетероструктур *n-TiN/p-CdTe/n-CdTe*, які володіють властивостями фототранзистора з непідключеною (плаваючою) базою. Показано, що у структурі *n-TiN/p-CdTe/n-CdTe* при зворотній напрузі на колекторному переході *p-CdTe/n-CdTe* за умов опромінення близьких до AM1 зі сторони емітера *n-TiN* спостерігається явище підсилення колекторного фотоструму прямим струмом прямо увімкненого гетеропереходу *n-TiN/p-CdTe*. Пряма напруга до гетеропереходу *n-TiN/p-CdTe* прикладається внаслідок позитивного заряду бази *p-CdTe* при освітленні. Проаналізовано фотоелектричні явища при освітленні гетероструктури *n-TiN/p-CdTe/n-CdTe*. Мета даної роботи оцінити практичне використання вперше створеної гетероструктури *n-TiN/p-CdTe/n-CdTe* в режимі роботи фототранзистора для створення сенсора освітленості із цифровим інтерфейсом для використання в мережевих системах контролю та управління. Обґрунтовано можливість використання виготовленого транзистора як цифрового сенсора освітленості для великих значень світлового потоку. Фототранзистор використовувався як первинний перетворювач для мікроконтролера в складі якого є функціональний блок операційного підсилювача. Фототранзистор і операційний підсилювач реалізують разом систему перетворювач фотострум-напруга. Дане рішення дозволяє використати внутрішній операційний підсилювач мікроконтролерів з однополярним живленням. Лінеаризація передаточних характеристик фототранзистора дозволяє використовувати мікроконтролери і з малими обчислювальними потужностями. Встановлено, що передаточні характеристики більш наближені до лінійних із збільшенням напруги між колектор-емітер фототранзистора. Сенсорний пристрій з використанням розробленого транзистора був зібраний на мікроконтролері серії PIC16F171, який містить операційний підсилювач дозволяє реалізувати цифровий інтерфейс USART для передачі виміряних даних світлового потоку. Реалізуючи безпровідний сенсор освітленості на модулі GB2530, базою якого є SoC (System-on-a-Chip), CC2530 дозволяє отримати мобільний пристрій. Обмін даними в радіоефірі відбувається відповідно до стандарту IEEE 802.15.4.

**КЛЮЧОВІ СЛОВА** фототранзистор, гетероструктура, мікроконтролер, освітленість.